A Novel Low-Power Linear Magnetostrictive Actuator With Local Three-Phase Excitation

Won-jong Kim, *Senior Member, IEEE*, and Ali Sadighi, *Student Member, IEEE*

***Abstract*—Development of a novel low-power linear magnetostrictive actuator is presented in this paper. The magnetostrictive material used here is Terfenol-D, which is an alloy of the formula $Tb_{0.3}Dy_{0.7}Fe_{1.92}$. In response to a traveling magnetic field inside the Terfenol-D element, it moves in the opposite direction with a peristaltic motion. The proposed design offers the flexibility to operate the actuator in various configurations including local and conventional three-phase excitation. In this paper, we demonstrate that the power consumption can be reduced significantly by the local excitation approach. A new force-transmission assembly incorporates spring washers to avoid the wear due to the sudden collision of the Terfenol-D element with the force-transmission assembly. The closed-loop control system was implemented using relay control, which resulted in an optimal closed-loop performance. The magnetostrictive motor has demonstrated a 410-N load capacity with a travel range of 45 mm, and the present maximum speed is 9 mm/min. The low speed is due to the local three-phase operation mode, and it could be increased to 60 mm/min by using the conventional three-phase operation. The maximum power consumption by the motor is 95 W.**

***Index Terms*—Finite-element methods, linear motors, magnetostriction, relay control systems.**

I. Introduction

ELECTRIC actuators have found many industrial applications and are extensively used in machine-tool sliding tables, semiconductor fabrication, helicopters, underwater vehicles, etc. [1], [2]. However, there are key applications that impose limits on the space required for the actuator or its power consumption. Meeting all these requirements is a challenging task, which motivates us to explore new technologies for the development of such actuators [3]. Hydraulic motors, despite their high force-generating capability, are not applicable where ample space is unavailable to accommodate the auxiliary parts of the hydraulic system such as a hydraulic pump. On the other hand, direct-drive linear electric motors could not compete with hydraulic ones in generating high forces, so rotary motors have been combined with gear reducers and ball or lead screws to increase the force capability. This approach, although effective in many situations, requires the added complexity of a speed reducer and introduces backlash.

Manuscript received December 11, 2008; revised April 1, 2009. First published June 30, 2009; current version published March 31, 2010. Recommended by Technical Editor I-M. Chen.

The authors are with the Department of Mechanical Engineering, Texas A&M University, College Station, TX 77843-3123 USA (e-mail: wjkim@tamu.edu; a_sadighi@tamu.edu).

Color versions of one or more of the figures in this paper are available online at http://ieeexplore.ieee.org.

Digital Object Identifier 10.1109/TMECH.2009.2024937

Considering these limitations, attention has been paid to smart materials as a new approach to develop novel actuators. Among them, giant magnetostrictive materials are in competition with piezoceramics [4], [5]. The magnetostrictive materials have found their place in specific applications such as low-voltage high-force actuators, high-power low-frequency transducers, and space cryogenic positioning. In other cases, piezoceramic actuators are employed because of their low power consumption and high output energy per unit mass [6].

Terfenol-D, which is an alloy of formula $Tb_{0.3}Dy_{0.7}Fe_{1.92}$, was developed in the 1950s at the Naval Ordnance Laboratory. This alloy has the highest magnetostriction of any alloy, up to 2000 ppm [7], [8]. Due to this small magnetostriction strain level, most of the available magnetostrictive actuators are capable of generating high forces within a very small range of actuation. One of the first studied applications of these materials was as a generator of force and motion for underwater sound sources [9], [10]. The first type of extended-range magnetostrictive motors was developed by Kiesewetter [11]. He conceived of the idea of generating the peristaltic motion with a Terfenol-D rod in a tight-fitting tube. The main drawback of his motor is wear, which would cause a loose contact between the Terfenol-D rod and the tube, leading to the loss of the force-generating capability.

To overcome this problem, Kim *et al.* constructed an extended-range linear magnetostrictive motor with double-sided three-phase stators [12]. Unlike the Kiesewetter's motor, they used Terfenol-D slab placed between two tight-fitting plates spring-loaded to maintain proper contact in spite of wear, thermal expansion, or motion. They demonstrated force-generating capability up to 140 N and a travel range of 25 mm. However, the power consumption was quite high due to applying conventional three-phase excitation in high frequency, which gave rise to eddy current loss [13].

We have developed a new type of linear magnetostrictive motor with a rectangular slab of Terfenol-D as the active element, as shown in Fig. 1. To overcome the power consumption limitation, we designed and implemented a novel configuration for coils. In this motor, the coils' magnetic axis coincides with the active element's magnetic axis, which aligns the direction of magnetic field inside the Terfenol-D slab better and results in higher magnetic flux density, and consequently, higher magnetostrictive strain. Furthermore, this design enables us to implement various operation modes such as the conventional multiphase excitation or a local multiphase excitation. The main focus of this paper is the local three-phase operation of the linear magnetostrictive motor. Since only 3 out of 24 coils are excited at

1083-4435/$26.00 © 2009 IEEE

Authorized licensed use limited to: Texas A M University. Downloaded on March 30,2010 at 17:22:11 EDT from IEEE Xplore. Restrictions apply.

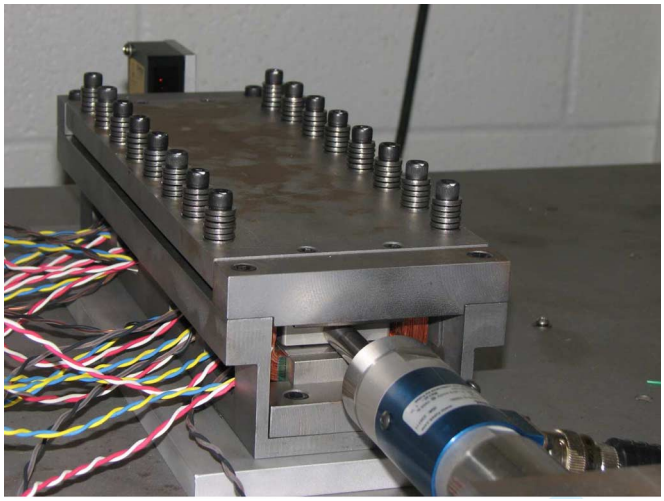

Fig. 1. Photograph of the linear magnetostrictive motor.

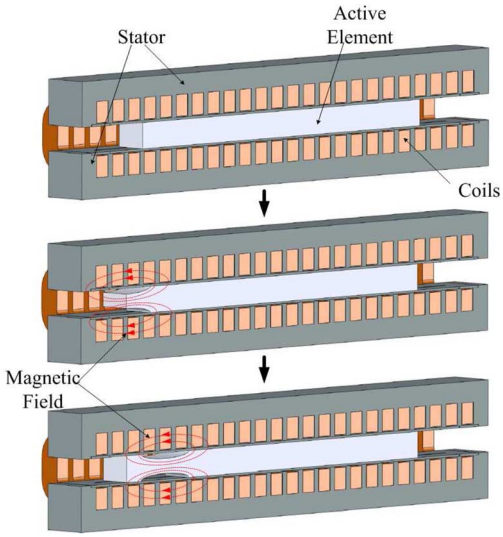

Fig. 2. Working principle of the linear magnetostrictive motor. By generating a traveling magnetic field through the active element, peristaltic motion is generated that results in overall displacement of the active element in the opposite direction of the traveling magnetic field.

TABLE I
COMPARISON AMONG DIFFERENT TYPES OF ACTUATORS

Actuator type	Actuation strain	Actuation stress (MPa)	Self-braking
Low-strain Piezoelectric	5×10^{-6}–3×10^{-5}	1–3	N/A
High-strain piezoelectric	5×10^{-5}–2×10^{-4}	4–9	N/A
Linear magnetostrictive actuator	0.16	1.025	Yes
Moving-coil transducer	1×10^{-2}–1×10^{-1}	4×10^{-3}–5×10^{-2}	N/A
Solenoid	1×10^{-1}–4×10^{-1}	4×10^{-2}–1×10^{-1}	N/A

each time in this operation mode, the power consumption could be reduced drastically. To date, we demonstrated the speed of 9 mm/min with the load capacity of 410 N and the travel range of 45 mm.

The actuation strain of the linear magnetostrictive actuator is limited only by the design of the actuator. In our current design, it is 0.16, which is far beyond the actuation strain in piezoelectric actuators. Although moving coil transducers and solenoid actuators are capable of generating high strains, their actual stress is lower than the linear magnetostrictive actuator [14]. Another feature that differentiates this actuator from other types is its self-braking capability, which enables it to hold its position when the power is cut off. A comparison among different types of actuators is given in Table I.

In Section II, we present the working principle and electromagnetic design of the linear magnetostrictive motor. Its mechanical design and fabrication are discussed in Section III. Section IV describes the power electronics and control system. The open-loop and closed-loop test results are then presented and discussed in Section V.

II. WORKING PRINCIPLE AND ELECTROMAGNETIC DESIGN

The working principle of the linear magnetostrictive motor is illustrated in Fig. 2. The main idea is to generate a traveling magnetic field inside the active element while keeping it under pressure. The active element is initially at rest in a tight fit inside a channel. A magnetic field could be generated by the means of the coils surrounding the active element. Two stators as shown are incorporated to enhance the magnetic flux density inside the active element. Now, if we move this magnetic field to the right, as it comes to interaction with the active element, it makes that portion of the active element elongate along the magnetic field lines. Since the volume of the active element is constant, this elongation will result in cross-sectional contraction of the active element, which releases the active element from its tight fit with the channel. As the magnetic field moves to the right, the neighboring portion of the active element expands while the last portion goes back to its original place and locks against the channel. When the magnetic field has passed completely through the active element length, the active element has moved to the left. By repeating this process over and over, peristaltic motion is generated resulting in overall displacement of the active element.

A. Underlying Theory

It was shown that the speed of a linear magnetostrictive motor is a function of the peak magnetostrictive strain, mechanical stress, and operation frequency [15]. For the linear magnetostrictive motor under local multiphase operation, the modified relationship between the motor speed and design parameters is

Authorized licensed use limited to: Texas A M University. Downloaded on March 30,2010 at 17:22:11 EDT from IEEE Xplore. Restrictions apply.

given by

$$v = N\,f\,p\left(\varepsilon_{\max} - \frac{F}{EA_T}\right) \tag{1}$$

where

N	number of phases (3);
f	local multiphase operation frequency (in hertz);
p	slot pitch (10.9 mm);
$\varepsilon_{\max}$	peak magnetostrictive strain under no-load condition;
F	external load (in newtons);
E	Young's modulus of Terfenol-D (35 GPa);
A_T	cross-sectional area of the Terfenol-D slab (400 mm^2).

Thus, the speed is proportional to the sum of the opposing strains from two different origins. One is the magnetostrictive strain denoted by $\varepsilon_{\max}$ and the other is mechanical strain denoted by F/EA_T resulted from the external load applied on the active element. The magnetostrictive strain is a function of applied magnetic field and could be calculated using the magnetostriction curve given in [16] and [17].

B. Electromagnetic Design

As seen before, the magnetostrictive strain has a direct impact on the speed and force capacity of the linear magnetostrictive motor. Hence, the main issue of the magnetic circuit design is to direct the magnetic flux as much as possible through the active element. By doing this, we would be able to lower the power requirements as well as to increase the force capacity. We employed a finite-element-analysis (FEA) approach for the design and optimization of the magnetic circuit [18], [19]. To do this, five different configurations for the key components such as stators, coils, and active element were proposed, and the FEA was run for each of them. Finally, by taking into account other design considerations such as ergonomics, ease of manufacturing, and assembly, a flat design with single set of coils was chosen.

The eddy current analysis was carried out for the frequencies as low as 0.1 Hz up to 60 Hz. After the FEA was performed, the core losses were evaluated by integrating the ohmic losses over the volume of the stators and the Tefenol-D slab. The core losses were found to be as low as 0.1 W in this range of frequencies, and the need for laminated stators could be eliminated. Optimization of motor parameters was carried out using FEA, in which the coil geometry, number of turns, slot size, and Terfenol-D geometry were selected. Due to the open-slot geometry, it was possible to use prefabricated coils. We incorporated 24 coils, each consisting of 273 turns of AWG #24 wire. The proposed design gives us the flexibility to connect these coils in various ways such as two-, three-, or four-phase configurations. The stator and coil geometries are depicted in Fig. 3(a) and (b). Table II summarizes the selected parameters for the linear magnetostrictive actuator.

FEA results for the magnetic field intensity inside the active element for the local three-phase operation is shown in Fig. 3(c). The magnetic circuit design resulted in a very uniform magnetic field intensity distribution throughout the cross section (A-A) of the Terfenol-D slab.

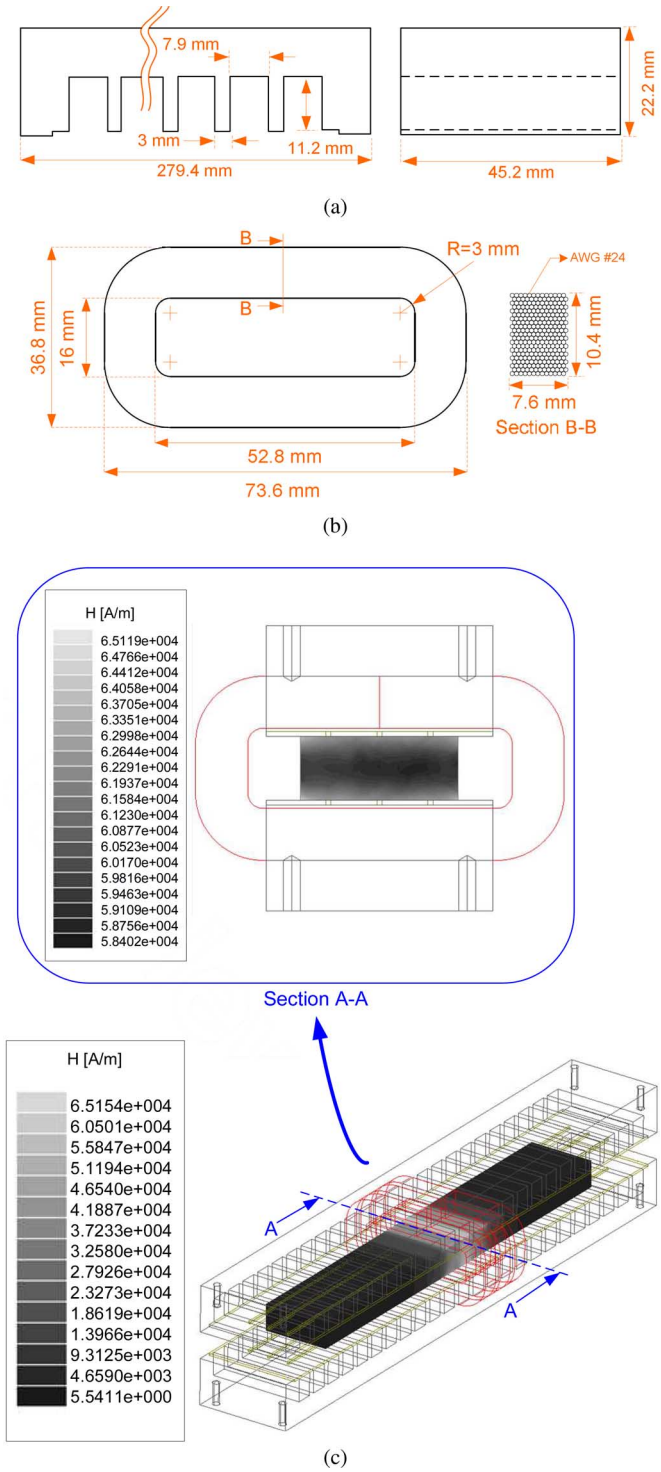

Fig. 3. (a) Stator slot geometry. (b) Coil geometry. (c) FEA was extensively used in the design and optimization of the linear magnetostrictive motor. Here, the magnetic field intensity distributions throughout the length of the active element and in its cross section are shown. The current in each coil is i =2.5 A.

III. Mechanical Design and Fabrication

A characteristic feature of magnetostrictive devices is that the resulting strains are on the order of hundredths to tenths of

Authorized licensed use limited to: Texas A M University. Downloaded on March 30,2010 at 17:22:11 EDT from IEEE Xplore. Restrictions apply.

TABLE II
PARAMETERS OF THE LINEAR MAGNETOSTRICTIVE ACTUATOR

Item	Specification
Overall mass	14.6 kg
Overall dimension	$86 \times 72 \times 320$ mm
Terfenol-D element dimension	$31.5 \times 12.7 \times 200$ mm
Number of coils	24
Wire gauge	AWG #24
Number of turns per coil	273
Coil resistance	4.28 Ω
Coil inductance	9.7 mH
Stator material	Nickel-Iron Alloy 49
Number of slots per stator	24

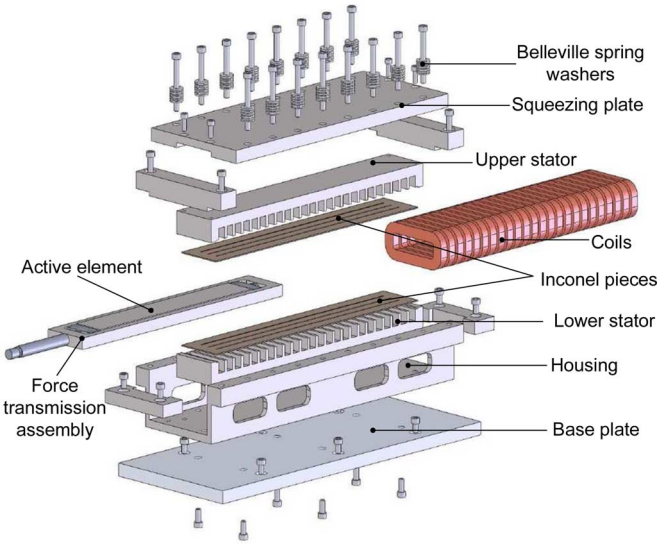

Fig. 4. Exploded view of the linear magnetostrictive motor.

millimeters. Therefore, special attention must be paid to tolerances in the construction. There is a need to manufacture or machine the magnetostrictive transmission parts with a tolerance level within a couple or tens of micrometers to achieve predictable performance. It is also important that all surfaces that transmit force and strain are flat and smooth. The smoothness requirement is normally within a couple of micrometers [20]. The mechanical design tasks involve the design of suitable housing, force-transmission assembly, squeezing mechanism, and stators.

A. Housing

The housing was designed considering the external load as well as the squeezing force that are transmitted to the housing structure. To remove the concerns over thermal distortion due to brazing or lack of precision in assembly, we machined the whole structure out of a solid piece of steel A36. The housing is shown in Fig. 4.

B. Stator

The stator in our design should have two main features. First, it should have high relative permeability to decrease the reluctance in the magnetic circuit. Second, it should be strong enough to withstand the shear forces due to external load as well as the pressure due to squeezing force. To meet these two criteria, we chose nickel–iron alloy 49 (EFI 50 by Ed Fagan, Inc.), which has very high relative permeability up to 100 000 along with good mechanical properties like yield stress of 154 MPa. Furthermore, a clearance of 0.5 mm is considered between the bottom of stator slots and the coil to avoid the coils' damage due to the normal squeezing pressure. As discussed earlier, we decided to make the stator by machining due to low core losses in low frequencies. The upper and lower stators are shown in Fig. 4.

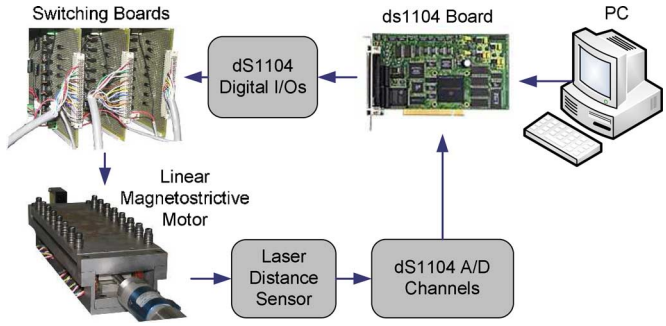

Fig. 5. Key components of the mechatronic system.

C. Force-Transmission Assembly

The rectangular slab of Terfenol-D is sandwiched between two stators, which are capped with 1-mm-thick pieces of Inconel-718 (Sheet 718 by Rolled Alloys). These thin pieces have very smooth surfaces with the surface roughness of 1 μm, which increases the friction force between the active element and the Inconel-718 pieces. These friction forces contribute to the reaction force required to move the active element against a load or to hold it in place. The relative permeability of Inconel-718 is as low as 1.001, which directs most of the magnetic flux through the active element. Since Terfenol-D is a brittle material, making holes or tapping would put it at risk. Hence, we designed a force-transmission assembly consisting of a stainless steel frame surrounding the Terfenol-D, as shown in Fig. 4. The generated force is transmitted to this frame through two rectangular ground pieces of stainless steel. Two sets of spring washers incorporated at each end assure a permanent contact between the Terfenol-D slab and these pieces. It also allows the expansion of the Terfenol-D slab in its longitudinal direction.

D. Squeezing Mechanism

To generate the required friction force between the Inconel-718 pieces and the Terfenol-D element, there should be a normal force applied to this assembly. This normal force is generated using 16 sets of Belleville washers and screws and transmitted through the squeezing plate, as shown in Fig. 4. We would be able to generate 6.66 kN normal force, which results in 4 kN maximum motor load considering the friction coefficient between Terfenol-D slab and Inconel-718 as 0.3.

Authorized licensed use limited to: Texas A M University. Downloaded on March 30,2010 at 17:22:11 EDT from IEEE Xplore. Restrictions apply.

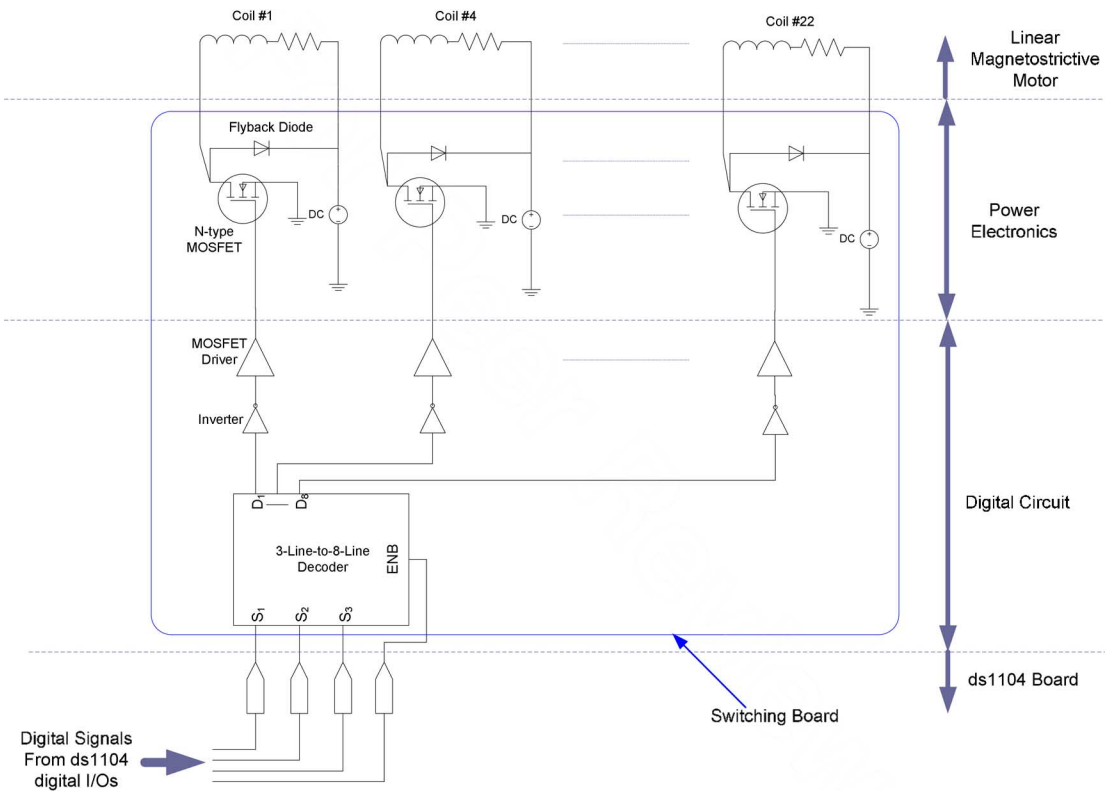

Fig. 6. Schematic diagram of digital circuit and power electronics for a single phase.

IV. Power Electronics and Control System

A. Power and Control Electronics

As mentioned earlier, the proposed design enables us to operate the linear magnetostrictive motor in various configurations including three-phase conventional operation and local multiphase operation. Here, we focus on the local three-phase operation.

The objective of power electronics here is to direct the required current to three adjacent coils, and then, move it to either side depending on the motor's motion direction. To achieve this goal, we designed and implemented three switching boards, each including eight power MOSFETs (model IRF3315Pbf by International Rectifier), eight MOSFET drivers (model TC4420 by Microchip), eight flyback diodes (model MUR405 by ON Semiconductor), three inverters, and one 3-line-to-8-line decoder. There is a dedicated power supply (model E3644A by Agilent) for each phase, which also monitors its voltage and current. Key components of this mechatronic system are shown in Fig. 5. A schematic diagram of different layers of the electronic system including the digital circuit and power electronics for a single phase is shown in Fig. 6.

The switching frequency of the power MOSFETs is controlled using the digital I/Os of a DSP board (model DS1104 by dSPACE). This DSP board is a 32-bit 250-MHz floating point DSP, with eight analog-to-digital (A/D) channels, eight digital-to-analog (D/A) channels, and 20 digital I/O channels. The motor shaft position is monitored with a laser distance sensor (model OADM 20I6460/S14F by Baumer Electric), which has a resolution of 5 μm and measuring distance ranging from 30 to 130 mm.

B. Open-Loop Tests

Various open-loop no-load tests were carried out at a constant frequency of 10 Hz. As mentioned earlier, this linear magnetostrictive motor was designed to work at low frequencies. Although we sacrifice its speed by operating the motor at low frequencies, its overall efficiency increases due to the reduction in core losses. In Fig. 7(a), the open-loop no-load motion profiles at the excitation frequency of 10 Hz and with varying peak phase currents from 0.6 to 2.55 A are shown. As the phase current increases, the profiles get closer to each other, which is due to the magnetic saturation inside the active element. The open-loop load test was performed at a phase peak current of 2.75 A and an excitation frequency of 5 Hz. The load was increased from 50 to 410 N, and the motion profiles are shown in Fig. 7(b). The nonlinearities seen in the trajectory of the actuator are brought about by the inherent nonlinearities in the nature of friction-based interaction between the active element and the Inconel pieces.

To verify the effectiveness of the model described by (1), the model-predicted speed was compared with the actual speed of the linear magnetostrictive actuator. To do this, the magnetic field intensity inside the active element was calculated at different currents using FEA. Then, the magnetostriction curve as in [17] was used to calculate the magnetostrictive strain. The results are illustrated in Fig. 8. The error between the

Authorized licensed use limited to: Texas A M University. Downloaded on March 30,2010 at 17:22:11 EDT from IEEE Xplore. Restrictions apply.

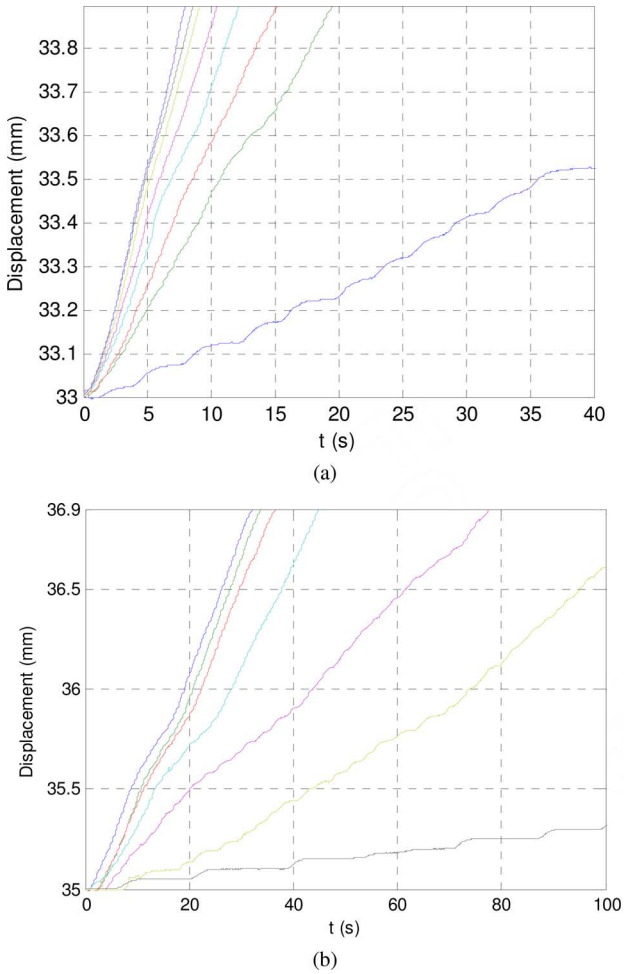

Fig. 7. (a) Open-loop no-load tests of the linear magnetostrictive motor excited at 10 Hz and with varying peak phase currents 0.6, 1.1, 1.35, 1.6, 1.85, 2.1, 2.3, and 2.55 A from the bottom. (b) Open-loop load tests of the linear magnetostrictive motor at the peak phase current of 2.75 A and the frequency of 5 Hz with varying loads 50, 100, 150, 200, 250, 300, and 410 N from the top.

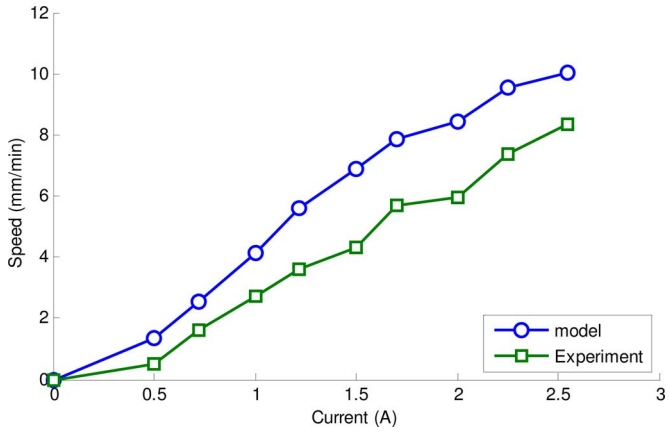

Fig. 8. Comparison between the model-predicted speed and the actual speed of linear magnetostrictive motor.

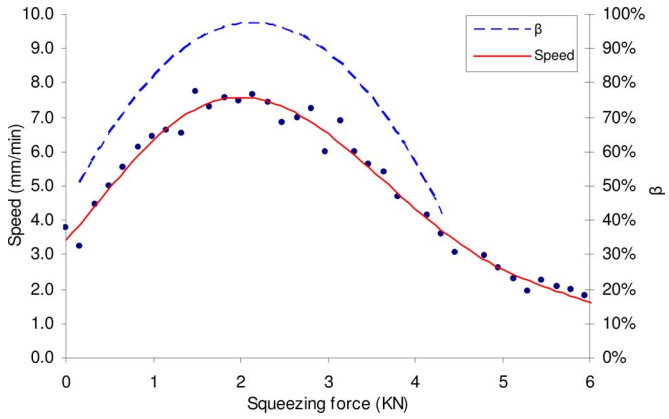

Fig. 9. Linear magnetostrictive actuator speed versus squeezing force.

model-predicted speed and the actual one is associated with the impact of surface roughness of the active element and also the Inconel pieces, which was not included in (1), the unavoidable misalignments during the assembly, and the deformation of stators and the Inconel pieces due to the application of the squeezing force. It is seen that as coil current increases, the error percentage decreases. This is due to the fact that at low currents, the magnetostrictive strains are very small. This results in very small lateral contraction of the active element, which causes the increase in friction force between the active element and the Inconel pieces. This friction force leads to a drop in the speed of the actuator at low currents. However, as the current increases, it facilitates the lateral contraction of the active element, which enables it to elongate without being opposed by the friction force imposed by the Inconel pieces.

The normal force applied by the squeezing mechanism affects both the speed and the blocking force of the linear magnetostrictive actuator. The increase in squeezing force boosts the friction force between the active element and the Inconel pieces, resulting in higher blocking forces. To verify the impact of the squeezing force on the speed of the actuator, it increased from 0 to 6000 N, and the speed of the actuator was recorded, as shown in Fig. 9. By increasing the squeezing force up to around 2000 N, the speed increases, and by further raising the squeezing force, the speed drops. This phenomenon could be explained in the following manner: in the beginning, by increasing the squeezing force, the Inconel intermediate plates come to closer contact with the Terfenol-D slab surface. This stops the Terfenol-D slab from slipping and increases speed. When the squeezing force goes beyond a certain limit, the magnetomechanical coupling [17] in Terfenol-D causes the magnetization of Terfenol-D slab to decrease, which consequently makes the magnetostrictive strains smaller and the actuator speed drop.

In Fig. 9, the dashed curve, $\beta(S)$, shows the drop in speed as a percentage of the maximum speed. The simple model introduced in (1) could now be enhanced to include the impact of squeezing force

$$v = \beta(S)\, N\, f\, p \left(\varepsilon_{\max} - \frac{F}{EA_T}\right) \tag{2}$$

where $\beta(S)$ is a function of squeezing force S. Since increasing the squeezing force beyond 4 kN results in very low speed of the actuator, which is not technically desirable, the experimental data were truncated above this point, and $\beta(S)$ was estimated

Authorized licensed use limited to: Texas A M University. Downloaded on March 30,2010 at 17:22:11 EDT from IEEE Xplore. Restrictions apply.

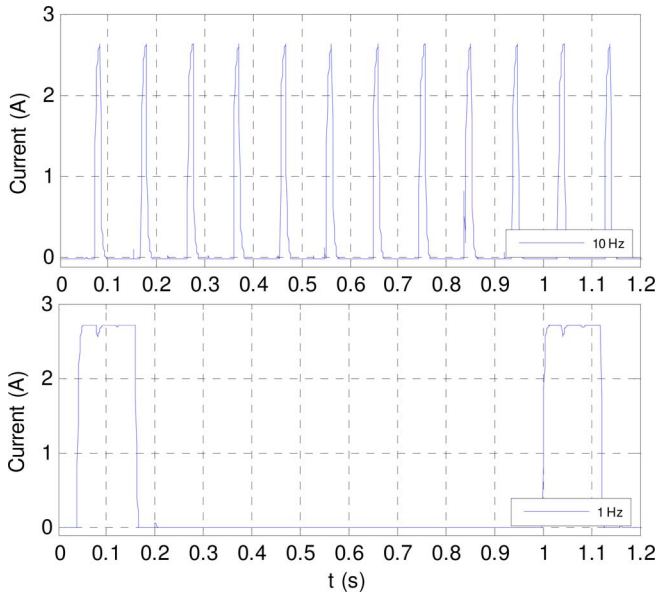

Fig. 10. Current profile in coils with phase voltage at 13 V and operation frequencies of 1 and 10 Hz.

by a second-order polynomial as

$$\beta(S) = -0.12S^2 + 0.51S + 0.43 \tag{3}$$

where S is the squeezing force in kilonewtons.

The phase currents were measured using Hall-effect-based current transducers (model LA 03-PB from LEM). The output voltages of the current transducers were sent to channels of the 16-bit A/D converter of the DSP board. The coil current profiles at a phase voltage of 13 V and operation frequencies of 1 and 10 Hz are shown in Fig. 10.

The power consumption of the linear magnetostrictive motor could then be calculated by integrating the current profile and using the following equation:

$$P = N\,V\left(\frac{1}{T_2 - T_1}\int_{T_1}^{T_2} i(t)\,dt\right) \tag{4}$$

where N is the number of coils, V is the phase voltage, and $i(t)$ is the instantaneous current in each coil. The maximum power consumption is then calculated at the phase voltage of 13 V to be 95 W.

V. Closed-Loop Control

We designed and successfully implemented a relay-based control system resulting in the minimum settling time with minimum overshoot. The schematic diagram of the closed-loop control system is shown in Fig. 11. The active element's position is monitored using the laser distance sensor and fed back to the controller. Based on the error value, the control signal is generated and sent via the digital I/O channels of the DSP board to the switching boards. Relay controllers have advantages over conventional linear controllers such as simplicity of design and fast response. In addition, unlike conventional linear controllers, a relay controller could be designed even when an exact model of the system is unavailable [21].

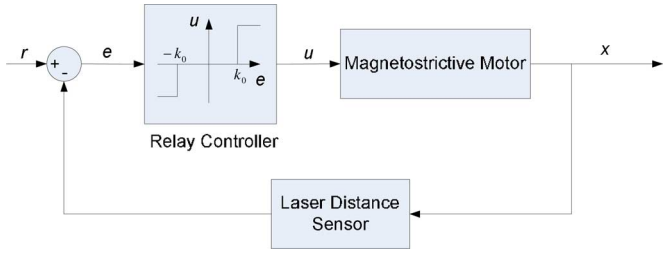

Fig. 11. Schematic diagram of the closed-loop control system.

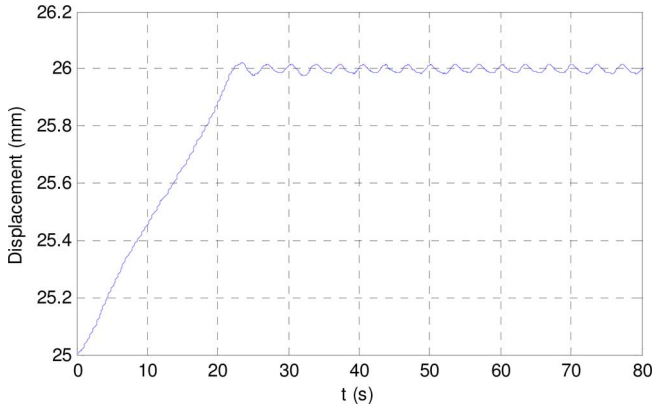

Fig. 12. 1-mm closed-loop step response with an excitation frequency at 10 Hz and a phase voltage of 5 V and the dead-zone threshold values of ± 0.005 mm.

To avoid self-oscillations [21] in the system response, we consider a relay controller with a dead zone defined as

$$u = \Phi(e) = \begin{cases} +1, & e > k_0 \\ 0, & -k_0 < e < k_0 \\ -1, & e < -k_0 \end{cases} \tag{5}$$

where u is the control signal and defines the actuator's movement direction by specifying the switching sequence of the MOSFET switches, and the threshold values $\pm k_0$ define the dead zone of the relay element. Due to the low speed of this actuator, to achieve the maximum possible speed, the phase voltage and the operation frequency are set at their maximum values. By doing so, the absolute value of the control signal is always maximized, which makes the motor move in either direction at the maximum speed.

We performed closed-loop tests with various values for k_0. As seen in Fig. 12, for the threshold value of 0.005 mm, the 1-mm closed-loop step response exhibited self-oscillations. We gradually increased the threshold value, and the self-oscillation frequency decreased as the threshold value increased. Finally, by choosing the threshold value as 0.02 mm, the self-oscillation disappeared. The 1-mm closed-loop step response with the dead-zone threshold value equal to 0.02 mm is shown in Fig. 13(a). There is no more oscillation in the response. By further increasing the threshold value, we might even remove the overshoot, but the downside would be the increase in steady-state error. Fig. 13(b) shows the capability of the designed controller in tracking a sinusoidal

Authorized licensed use limited to: Texas A M University. Downloaded on March 30,2010 at 17:22:11 EDT from IEEE Xplore. Restrictions apply.

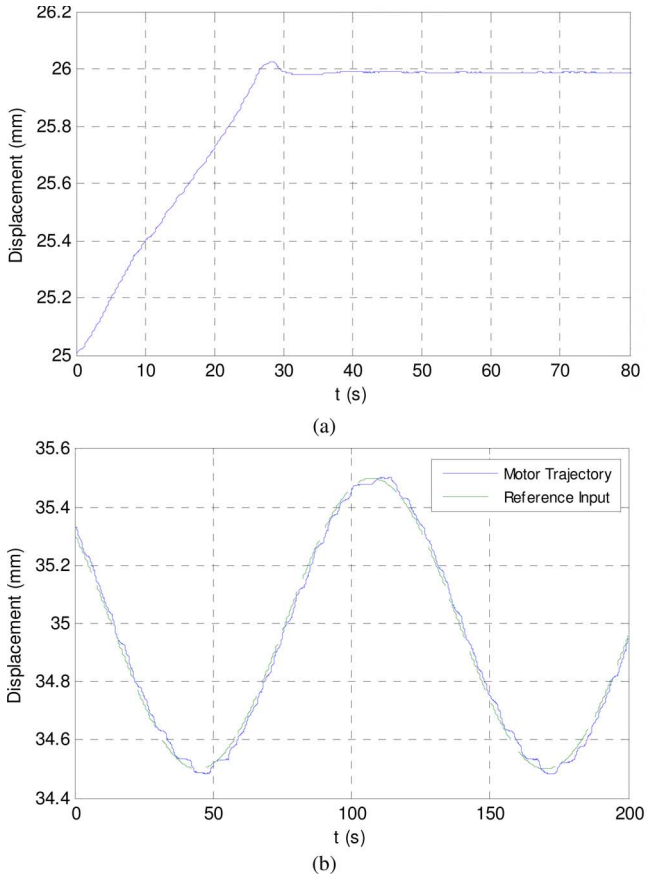

Fig. 13. (a) Same step response with the dead-zone threshold values of ± 0.02 mm. (b) Closed-loop response to a sinusoidal reference input with an amplitude of 0.5 mm and frequency of 0.05 rad/s.

reference input with an amplitude of 0.5 mm and frequency of 0.05 rad/s.

VI. Conclusion

We designed and constructed a low-power linear magnetostrictive actuator. FEA was used to design and optimize its magnetic circuit. Our design allowed the flexibility to operate it in various configurations depending on the type of applications. A local three-phase operation mode was developed in response to the requirements in the applications where power consumption is a limiting factor. The power electronics was developed for this novel linear actuation system, and an effective relay-based controller was designed and implemented. The linear magnetostrictive motor in the local three-phase operation mode demonstrated its force-generating capability of 410 N and travel range of 45 mm with power consumption of 95 W. The relay-based closed-loop control of the linear magnetostrictive motor resulted in the positioning accuracy of 20 μm. In comparison with conventional piezoelectric actuators, it could generate much higher actuation strains. It has higher actuation stresses in comparison with solenoid and moving-coil transducers. In this paper, a simple model of this novel linear magnetostrictive actuator was presented, which facilitated the design process. However, more comprehensive models containing the nonlinearities present in the system could lead to higher-performance designs in the development of a next-generation actuator.

Acknowledgment

The authors would like to thank Prof. H. A. Toliyat and Dr. S. Talebi of Texas A&M University for their advice on power electronics and magnetic circuit design. They also thank Y. H. Kim for assistance in fabrication of mechanical parts.

References

[1] H. Son and K.-M. Lee, "Distributed multipole models for design and control of PM actuators and sensors," *IEEE/ASME Trans. Mechatronics*, vol. 13, no. 2, pp. 228–238, Apr. 2008.
[2] P. Karutz, T. Nussbaumer, W. Gruber, and J. W. Kolar, "Novel magnetically levitated two-level motor," *IEEE/ASME Trans. Mechatronics*, vol. 13, no. 6, pp. 658–668, Dec. 2008.
[3] M. Ataka, B. Legrand, L. Buchaillot, D. Collard, and H. Fujita, "Design, fabrication, and operation of two-dimensional conveyance system with ciliary actuator arrays," *IEEE/ASME Trans. Mechatronics*, vol. 14, no. 1, pp. 119–125, Feb. 2009.
[4] R. Merry, N. de Kleijn, M. van de Molengraft, and M. Steinbuch, "Using a walking piezo actuator to drive and control a high-precision stage," *IEEE/ASME Trans. Mechatronics*, vol. 14, no. 1, pp. 21–31, Feb. 2009.
[5] E. Steltz and R. S. Fearing, "Dynamometer power output measurements of miniature piezoelectric actuators," *IEEE Trans. Mechatronics*, vol. 14, no. 1, pp. 1–10, Feb. 2009.
[6] F. Claeyssen, N. Lhermet, and T. Maillard, "Magnetostrictive actuators compared to piezoelectric actuators," in *Proc. SPIE Conf. Smart Struct. Eng. Technol.*, 2003, vol. 4763, pp. 194–200.
[7] F. Claeyssen, N. Lhermet, and G. Grosso, "Giant magnetostrictive alloy actuators," *J. Appl. Electromagn. Mater.*, vol. 5, pp. 67–73, 1994.
[8] F. Claeyssen, N. Lhermet, R. L. Letty, and P. Bouchilloux, "Actuators, transducers and motors based on giant magnetostrictive materials," *J. Alloys Compounds*, vol. 258, pp. 61–73, Aug. 1997.
[9] J. Goldie, M. J. Gerver, J. Oleksy, G. P. Carman, and T. A. Duenas, "Composite Terfenol-D sonar transducers," in *Proc. SPIE Conf. Smart Mater. Technol.*, Mar. 1999, vol. 3675, pp. 223–234.
[10] L. Kvarnsjo, "Underwater acoustic transducers based on Terfnenol-D," *J. Alloys Compounds*, vol. 258, pp. 123–125, Aug. 1997.
[11] L. Kiesewetter, "The application of Terfenol in linear motors," in *Proc. 2nd Int. Conf. Giant Magnetostrictive Alloys*, 1988, pp. 1–11.
[12] W.-J. Kim, J. H. Goldie, M. J. Gerver, J. E. Kiley, and J. R. Swenbeck, "Extended-range linear magnetostrictive motor with double-sided three-phase stators," *IEEE Trans. Ind. Appl.*, vol. 38, no. 3, pp. 651–659, May/Jun. 2002.
[13] D. Kendall and A. R. Piercy, "The frequency dependence of eddy current losses in Terfenol-D," *J. Appl. Phys.*, vol. 73, pp. 6174–6176, May 1993.
[14] J. E. Huber, N. A. Fleck, and M. F. Ashby, "The selection of mechanical actuators based on performance indices," *Math., Phys. Eng. Sci.*, vol. 453, pp. 2185–2205, Oct. 1997.
[15] J. Goldie, M. J. Gerver, J. Kiley, and J. R. Swenbeck, "Observations and theory of Terfenol-D inchworm motors," in *Proc. SPIE 5th Annu. Int. Symp. Smart Struct. Mater.*, Mar. 1998, vol. 3329, pp. 780–785.
[16] ETREMA Products Inc. (2009). [Online]. Available: http://www.etrema-usa.com
[17] W. Mei, T. Umeda, S. Zhou, and R. Wang, "Magnetostriction of grain-aligned $\mathrm{Tb_{0.3}Dy_{0.7}Fe_{1.95}}$," *J. Alloys Compounds*, vol. 224, pp. 76–80, Jun. 1995.
[18] F. Claeyssen, R. Le Letty, N. Lhermet, R. Bossut, and B. Hamonic, "Analysis of magnetostrictive inchworm motors using finite element modeling," in *Proc. Elsevier Conf. Magnetoelastic Effects Appl.*, 1993, pp. 161–167.
[19] M. E. H. Benbouzid, G. Reyne, and G. Meunier, "Finite element modeling of magnetostrictive devices: Investigations for the design of the magnetic circuit," *IEEE Trans. Magn.*, vol. 31, no. 3, pp. 1813–1816, May 1995.
[20] G. Engdahl, *Handbook of Giant Magnetostrictive Materials*. San Diego, CA: Academic, 2000.
[21] Y. Z. Tsypkin, *Relay Control Systems*. Cambridge, MA: Cambridge Univ. Press, 1984.

Authorized licensed use limited to: Texas A M University. Downloaded on March 30,2010 at 17:22:11 EDT from IEEE Xplore. Restrictions apply.

Won-jong Kim (S'89–M'97–SM'03) received the B.S. (*summa cum laude*) and M.S. degrees in control and instrumentation engineering from Seoul National University, Seoul, Korea, in 1989 and 1991, respectively, and the Ph.D. degree in electrical engineering and computer science from Massachusetts Institute of Technology (MIT), Cambridge, in 1997.

Since 2000, he has been with the Department of Mechanical Engineering, Texas A&M University (TAMU), College Station, where he is currently an Associate Professor and the Holder of the Dietz Career Development Professorship II. He was with SatCon Technology Corporation, Cambridge, MA, for three years. His current research interests include the analysis, design, and real-time control of mechatronic systems, networked control systems, and nanoscale engineering and technology. He is the holder of three U.S. patents on precision positioning systems. He is an Associate Editor of the *ASME Journal of Dynamic Systems, Measurement and Control* and the *International Journal of Control, Automation, and Systems*.

Dr. Kim was the recipient of Korean Institute of Electrical Engineers' Student Paper Contest Grand Prize in 1988, the Samsung Electronics' Humantech Thesis Gold Prize for his MIT dissertation in 1997, the National Aeronautics and Space Administration (NASA) Space Act Award in 2002, and the 2005 Professional Engineering Publishing Award for the best paper published in the *Journal of Engineering Manufacture* in 2004. He was also a semifinalist of NIST's Advanced Technology Program Competition in 2000. He was appointed a Select Young Faculty Fellow by the TAMU College of Engineering and the Texas Engineering Experiment Station twice in 2003 and 2005. He received the British Petroleum Teaching Excellence Award by the TAMU College of Engineering in 2006. He is a member of Pi Tau Sigma and the American Society of Mechanical Engineers (ASME). He is a Technical Editor of the IEEE/ASME TRANSACTIONS ON MECHATRONICS.

Ali Sadighi (S'08) was born in Yazd, Iran, in 1978. He received the B.S. degree from Sharif University of Technology, Tehran, Iran, in 2000, and the M.S. degree from K. N. Toosi University of Technology, Tehran, in 2003, both in mechanical engineering. He is currently working toward the Ph.D. degree in mechanical engineering at Texas A&M University, College Station.

From 2003 to 2006, he was with MAPNA, Tehran, as a Design Engineer. His current research interests include analysis, design, and real-time control of electromechanical systems.

Mr. Sadighi is a Student Member of the American Society of Mechanical Engineers (ASME) and the Phi Kappa Phi.

Authorized licensed use limited to: Texas A M University. Downloaded on March 30,2010 at 17:22:11 EDT from IEEE Xplore. Restrictions apply.